IOP Conf. Series: Journal of Physics: Conf. Series **932** (2017) 012022 doi:10.1088/1742-6596/932/1/012022

Systematic study of magnetar outbursts

F Coti Zelati[1,2,3], N Rea[1,2], J A Pons[4], S Campana[3] and P Esposito[2]

[1] Institute of Space Sciences (ICE, CSIC–IEEC), Campus UAB, Carrer de Can Magrans, S/N, 08193, Barcelona, Spain
[2] Anton Pannekoek Institute for Astronomy, University of Amsterdam, Postbus 94249, NL-1090-GE Amsterdam, The Netherlands
[3] INAF – Osservatorio Astronomico di Brera, via Bianchi 46, I-23807 Merate (LC), Italy
[4] Departament de Física Aplicada, Universitat d'Alacant, Ap. Correus 99, E-03080 Alacant, Spain

E-mail: cotizelati@ice.csic.es

Abstract. We present the results of the systematic study of all magnetar outbursts observed to date through a reanalysis of data acquired in about 1100 X-ray observations. We track the temporal evolution of the luminosity for all these events, model empirically their decays, and estimate the characteristic decay time-scales and the energy involved. We study the link between different parameters (maximum luminosity increase, outburst peak luminosities, quiescent X-ray and bolometric luminosities, energetics, decay time-scales, magnetic field, spin-down luminosity and age), and reveal several correlations between different quantities. We discuss our results in the framework of the models proposed to explain the triggering mechanism and evolution of magnetar outbursts. The study is complemented by the Magnetar Outburst Online Catalog (http://www.magnetars.ice.csic.es), an interactive database where the user can plot any combination of the parameters derived in this work and download all reduced data.

1. Introduction

Magnetars are strongly magnetized (up to $B \sim 10^{14} - 10^{15}$ G) isolated X-ray pulsars with spin periods $P \sim 2 - 12$ s and secular spin-down rates $\dot{P} \sim 10^{-15}$–10^{-11} s s^{-1}, whose emission is ultimately powered by the decay and the instability of their ultra-strong magnetic field [1–3]. Magnetars unpredictably undergo outbursts, in which the persistent X-ray luminosity increases by a factor of $\sim 10 - 1000$ up to $\sim 10^{35} - 10^{36}$ erg s^{-1}, and declines back to the quiescent level on a time-scale ranging from a few weeks up to several years.

Magnetar outbursts are likely triggered by local internal magnetic stresses that deform irreversibly part of the stellar crust and convert mechanically its magnetic energy into heat [4]. Part of the released heat is then conducted up to the surface and radiated, producing the observed thermal emission. The crustal displacements also implant a strong twist in the magnetosphere, likely confined to a bundle of current-carrying closed field lines anchored in the crust. The charged particles flowing along the field lines of the twisted bundle hit the star, providing an additional source of heat [5]. According to this scenario, the outburst evolution is regulated by the dissipation of the twist: the spatial extent of the bundle gets gradually more limited, the area on the star surface hit by the charges shrinks and the luminosity decreases.

Here we present the results of a systematic and homogeneous analysis of the spectral properties for 23 outbursts (from the very first active phases throughout their decays) from

17 magnetars using all the available data acquired by the *Swift*, *Chandra* and *XMM–Newton* X-ray observatories, as well as data collected in a handful of observations by the instruments aboard *Beppo*SAX, *ROSAT* and *RXTE*. This sums up to about 1100 observations, for a total dead-time corrected on source exposure time of more than 12 Ms.

2. Data analysis

We adopted standard procedures to extract source and background spectra and create or assign the response and auxiliary files starting from the raw *Swift*, *XMM–Newton* and *Chandra* data files publicly available. We performed the spectral analysis separately for data of different instruments (owing to known cross-calibration uncertainties) within XSPEC (v. 12.9.0; [6]).

To model the continuum emission, we fitted either a blackbody, a power-law, a blackbody plus a power-law, the superposition of two blackbodies or a resonant cyclotron scattering model (NTZ; [9,10]) to the spectral data sets. The NTZ model accounts for the repeated resonant cyclotron up-scatterings of thermal photons from the star surface onto the charges flowing in a twisted magnetosphere, and is based on three-dimensional Monte Carlo simulations. The topology of the magnetic field is assumed to be a globally twisted, force-free dipole in the model, and its parameters are the surface temperature (assumed to be the same over the whole surface), the bulk motion velocity of the charged particles in the magnetosphere (assumed constant through the magnetosphere), the twist angle and a normalization constant. In a few cases, the higher statistics quality available from *XMM–Newton* observations allowed us to probe more complicated models, such as the sum of three black-body components. The photo-electric absorption by the interstellar medium along the line of sight was described via the Tuebingen-Boulder model with cross-sections from [7] and chemical abundances from [8].

The absorbed and unabsorbed fluxes for the additive components and the total one (all in the 0.3–10 keV energy range) were computed for each fitted spectrum. Unabsorbed fluxes were converted to luminosities (as measured by an observer at infinity) assuming isotropic emission and the most reliable value for the distance of the source (e.g., [1]).

Figure 1 shows the temporal decays of the bolometric luminosities for all outbursts. We refer each curve to the epoch of the outburst onset, defined as the time of the first burst detection from the source, or of the giant flare in the case of SGR 1806−20. For XTE J1810−197 and 1E 1048.1−5937, for which no bursts were detected, we adopted the epoch of the observation where an increase in the X-ray flux was first measured as the reference epoch. Our bolometric luminosities do not take into account the emission of magnetars in the hard X-ray range, which in some sources was observed to give a relevant contribution to the total luminosity, especially during the initial phases (weeks) of the outburst (e.g., [11]). However we note that, if we consider all the hard X-ray observations of magnetar outbursts performed so far, our values for the bolometric fluxes are underestimated for a few sources (SGR 1806−20, 1E 2259+586, 1E 1547−5408, SGR 1745−2900, SGR 1935+2154, PSR J1119−6127 and 1E 161348−5055) mainly only at the outburst peak, yielding negligible differences in the estimated outburst energetics and decay timescale (see below).

2.1. Outburst decay time-scale and energetics

We modelled the decays of the X-ray luminosities of the single spectral components and of the bolometric luminosities using a constant (representing the quiescent level) plus one or more exponential functions. The number of required exponential functions was evaluated by means of the F-test, i.e., an additional exponential function was included only if it yielded an improvement in the fit of at least 3σ. L_q was fixed at the quiescent value or, in cases of non detections, constrained to be lower than the upper limit.

We estimated the outburst energy by integrating the best-fitting model for the bolometric light curves over the whole duration of the event, and extrapolating it to the quiescent value for

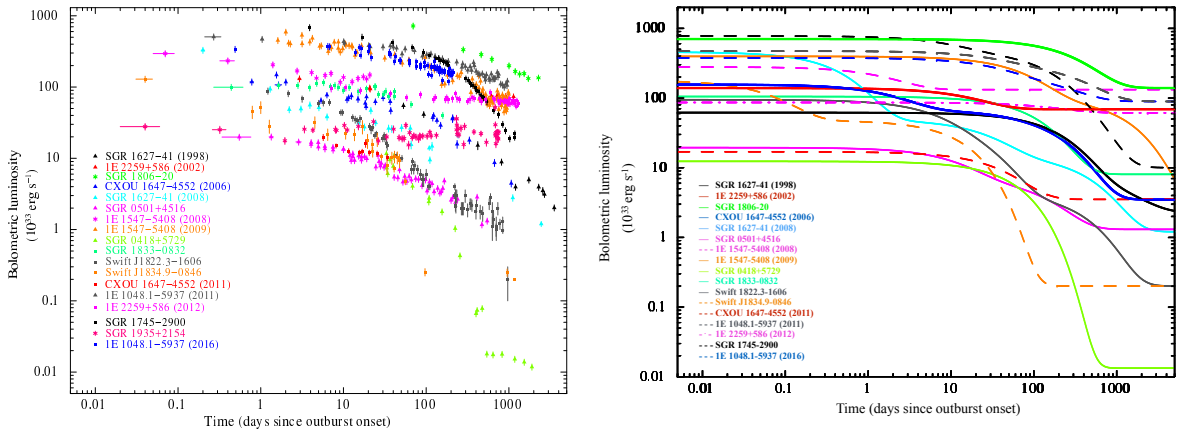

Figure 1. Left-hand panel: temporal evolution of the bolometric (0.01–100 keV) luminosities for the most densely monitored magnetar outbursts re-analysed in the present work. Right-hand panel: models reproducing the temporal evolution of the bolometric luminosities.

the cases where the observational campaign was not extended enough to follow completely the return to the pre-outburst state. For the sources that are still recovering from their outbursts (i.e., 1E 1547−5408, SGR 1745−2900, 1E 1048.1−5937, PSR J1119−6127 and 1E 161348−5055), we assumed no changes in the decay pattern down to quiescence for the estimate of the time-scales and energetics (in these cases the values derived should be considered only as upper limits).

3. Correlations

Our systematic analysis allows us to search for correlations between different parameters for all sources of our sample and their outbursts. Table 1 lists the significance for the correlations according to both the Spearman and Kendall τ rank correlation tests, and also reports on the shape of the correlation according to a power-law regression test. Figure 2 shows the results for some of the (anti-)correlations unveiled from our systematic study. To have a more complete sample, we also included SGR 1900+14, 4U 0142+61 and 1E 1841−045, for which re-brightenings or subtle variations around their persistent activity were reported throughout the last 15 years, as well as the other few magnetars (black stars), the central compact objects (grey crosses), the rotation-powered pulsars with evidence for a clear thermal component (red diamonds) and the X-ray dim isolated neutron stars (orange crosses) already reported by [12]. PSR J1119−6127 and the magnetars XTE J1810−197, 1E 1547−5408 and SGR 1745−2900, for which radio pulsed emission has been detected [13–15], are marked by black circles. Upper and lower limits are indicated by black arrowheads.

4. Results

We carried out the first systematic study of all sources experiencing magnetar-like outbursts up to the end of 2016, and for which extensive X-ray monitoring campaigns of their outbursts are available. We re-analysed in a coherent way about 1100 X-ray observations, adopting the same assumptions and spectral models throughout the whole sample. This work allows us to study possible correlations and anticorrelations between several different combinations of parameters, and put the results in the context of the models proposed to explain the triggering mechanism and evolution of magnetar outbursts.

Table 1. Results of the search for (anti-)correlations between different parameters. Letters in parentheses indicate the case of a correlation (c) or an anti-correlation (a). Values for the power-law index indicate the shape of the (anti-)correlation, and were estimated via a power-law regression test.

First parameter	Second parameter	Corr/Anticorr, Significance (σ) (c) or (a), Spearman / Kendall τ	PL index
Quiescent X-ray luminosity	Maximum luminosity increase	(a) , 5.7 / 4.9	-0.7
Dipolar magnetic field	Quiescent bolometric luminosity	(c) , 3.2 / 2.9	2.0
Dipolar magnetic field	Peak luminosity	(c) , 2.5 / 2.4	0.5
Dipolar magnetic field	Outburst energy	(c) , 3.7 / 3.3	1.0
Characteristic age	Outburst energy	(a) , 3.3 / 3.0	-0.4
Peak luminosity	Outburst energy	(c) , 4.0 / 3.7	1.4
Outburst energy	Decay time-scale	(c) , 3.9 / 3.6	0.5

4.1. On the relation between the outburst luminosity increase and the quiescent luminosity
It was already noted a few years ago that magnetars characterized by low quiescent luminosities ($L_q \sim 10^{31-33}$ erg s^{-1}) experience large luminosity increases when in outburst, whereas highly luminous sources in quiescence ($L_q \sim 10^{34-35}$ erg s^{-1}) undergo only subtle enhancements in luminosity during their outbursts ([16]; see also the top-left panel of Figure 2). This discovery also clarified that the distinction between 'transient' and 'persistent' sources within the magnetar population is deceptive, and only dependent on the initial quiescent luminosity of each source.

The anticorrelation between magnetars quiescent luminosities and their luminosity increases during outbursts is observed at a significance of 5.7σ (according to the Spearman test; see Table 2). This result suggests the existence of a limiting luminosity of $\sim 10^{36}$ erg s^{-1} for magnetar outbursts (regardless of the quiescent level of the source), and was interpreted in the framework of the internal crustal heating model as the observational manifestation of the self-regulating effect resulting from the strong temperature-dependence of the neutrino emissivity [16]: the surface photon luminosity for injected energies larger than $\sim 10^{43}$ erg reaches a limiting value of $\sim 10^{36}$ erg s^{-1} because the crust is so hot that most of the energy is released in the form of neutrinos before reaching the star surface. The observed anticorrelation is expected also in the scenario of the untwisting magnetospheric bundle, where the maximum theoretically expected luminosity might be of a few 10^{36} erg s^{-1} even for the generous case of a twist with $\psi \sim 1$ rad affecting a large part of the magnetospheric volume. The generally lower values observed for the peak luminosity are interpreted, in this model, as a consequence of the limited size of the current bundle and the twist [5].

The epoch of the outburst onset was defined throughout this study as the time of the first burst detection from the source (mostly with *Swift* BAT or *Fermi* GBM), or of the giant flare in the case of SGR 1806−20. This might represents a somewhat arbitrary choice, because the increase of the persistent flux during the time interval preceding the detection of magnetars bursting activity is usually missed by X-ray instruments. However, given the large sample, and the clear trend observed over several orders of magnitude, we do not expect to measure significantly different values for the outburst peak luminosity.

Different estimates on the time-scale of the luminosity increase were proposed in the past years. The internal crustal cooling models [16] show that the internal heat wave takes some time to propagate from the location in the crust where the energy is injected up to the surface layers. Therefore, the luminosity increase is not instantaneous but relatively fast, and might range from a few hours up to a few days depending on the depth of the region where heat is released. On the other hand, simplified one-dimensional models [17] show that the time-scale

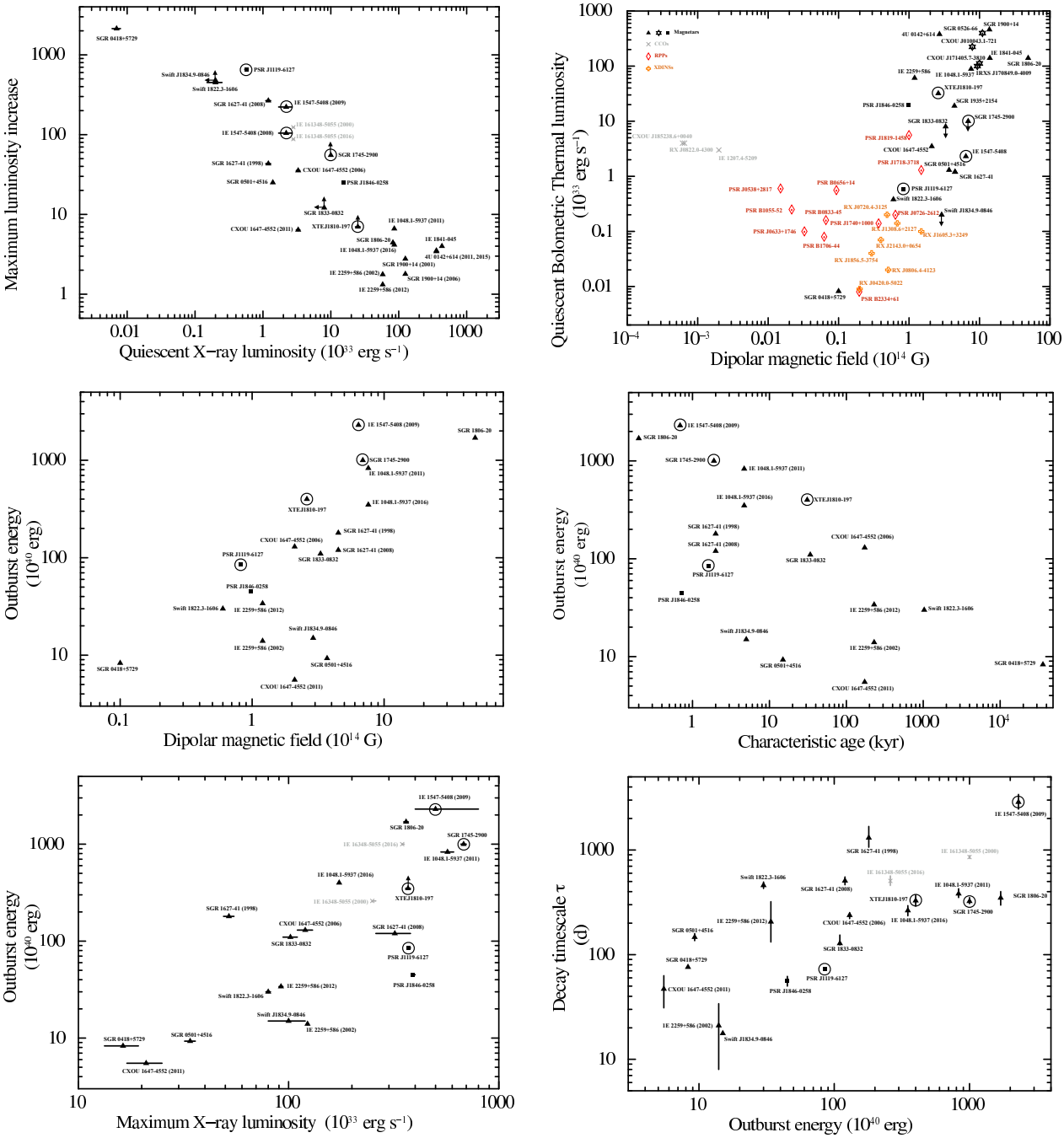

Figure 2. From left to right, top to bottom: quiescent X-ray luminosity versus maximum X-ray luminosity increase; quiescent bolometric luminosity relative to the thermal component versus the dipolar component of the magnetic field; total energy released during the outburst as a function of the dipolar component of the magnetic field; total energy released during the outburst as a function of the characteristic age; total energy released during the outburst versus maximum X-ray luminosity at the peak of the outburst; decay time-scale as a function of the total energy released during the outburst.

of magnetospheric twisting by a large thermoplastic wave (corresponding to the rise time of the outburst) can span from days to weeks. Within the large uncertainties, both models are compatible with a typical rise time of a few days.

4.2. On the quiescent luminosity versus the dipolar magnetic field

The top-right panel of Figure 2 shows the quiescent thermal bolometric luminosity as a function of the surface dipolar magnetic field. We observe a significant correlation (3.2σ according to the Spearman test) when including all sources belonging to the different classes considered in this study. The correlation is even more significant (3.9σ) after excluding the central compact objects, and is naturally explained in terms of magnetic field decay and Joule heating [18,12]. The central compact objects clearly depart from the general trend. The peculiar behavior of these objects might be explained in the framework of the 'hidden magnetic field' scenario: hypercritical accretion onto the neutron star surface during the initial stages of the star life can bury a magnetic field of a few 10^{13} G into the inner crust, yielding a strength for the external magnetic field that is significantly lower than the internal 'hidden' magnetic field. The large luminosity observed for these objects is most probably due to the toroidal and higher order multipolar components of the magnetic field trapped inside the crust [19–22]. The magnetic field might eventually re-emerge, after a few thousand years, settling on a value comparable to that at birth. If this picture is correct, we would expect a 'shift' of the central compact objects towards the right in the quiescent luminosity versus dipolar magnetic field diagram, as the CCOs get older. Some of the rotation powered pulsars also depart slightly from the observed trend (e.g., PSR J0538+2817, PSR B1055−52 and PSR J0633+1746). This might be possibly due to an additional contribution to the surface heating from slamming particles onto the stellar surface, as typically observed for pulsars with a high rotational energy loss rate.

The shape of the correlation can be approximated as $L_{q,bol} \propto B^2_{p,dip}$, in line with the dependence reported in a previous study using a reduced sample of sources [23].

4.3. On the dipolar magnetic field versus the outburst properties

We investigated possible correlations between the strength of the surface dipolar magnetic field and all the outburst parameters derived in the present study. There is no clear correlation between the magnetic field and either the outburst peak luminosity or the decay time-scale. Moreover, in a few cases the same source was observed to undergo two different outbursts with distinct properties. The correlation between the magnetic field and the outburst energetics is more evident (3.4σ according to the Spearman test; see the middle-left panel of Figure 2), and supports the idea that the energy reservoir of the outbursts is mainly provided by the dissipation of the magnetic field. We observe a sort of limiting energy as a function of age (see the middle-right panel of Figure 2). Young magnetars tend to experience more energetic outbursts than older magnetars, a characteristic that can be explained simply in terms of field decay. Previous estimates on the expected energetics distribution did not find a significant dependence of the energy of the events with age, but the fact that magnetic field decay limits the energy budget available for old magnetars, compared to young sources [24].

4.4. On the outburst energy versus other properties

The outburst energy correlates with the peak luminosity (at a significance of 4.0σ according to the Spearman test; see the bottom-left panel of Figure 2), but not with the quiescent X-ray luminosity ($< 2\sigma$). These results suggest that a larger luminosity at the peak of the outburst results in a larger energy released during the outburst event, regardless of the quiescent level of the source, and indicate similar patterns for the decay curves of magnetar outbursts. This is expected in both internal crustal cooling and untwisting bundle scenarios, since it only reflects the normalization of the decay curve.

The decay time-scale significantly correlates with the energetics (at a significance of 3.9σ according to the Spearman test; see the bottom-right panel of Figure 2): the longer the outburst, the more energetic. This suggests again that the decay pattern is similar from outburst to outburst. For example, we never observe a magnetar undergoing a rather weak outburst and then returning to quiescence over an extremely long time interval, or a magnetar showing an extremely powerful outburst and then rapidly decaying back to quiescence.

Acknowledgments

We are indebted to Santiago Serrano Elorduy and Martin Folger from the Institute of Space Sciences (CSIC–IEEC) for designing the Magnetar Outburst Online Catalogue. The scientific results reported in this study are based on observations obtained with *XMM–Newton*, an ESA science mission with instruments and contributions directly funded by ESA Member States and NASA, and *Swift*, a NASA/UK/ASI mission. This research has made extensive use of software provided by the *Chandra X-ray Center* in the application package CIAO. FCZ acknowledges funding in the framework of the Netherlands Organization for Scientific Research (NWO) Vidi award (PI: N. Rea) and the European COST Action MP1304 (NewCOMPSTAR), and is also supported by grants AYA2015-71042-P and SGR2014-1073.

References

[1] Olausen S A and Kaspi V M 2014 *Astrophys. J. Suppl. Ser.* **212** 6
[2] Turolla R, Zane S and Watts A 2015 *Rep. Prog. Phys.* **78** 116901
[3] Kaspi V M and Beloborodov A M 2017 *Annu. Rev. Astron. Astrophys.* in press
[4] Beloborodov A M and Levin Y 2014 *Astrophys. J.* **794** L24
[5] Beloborodov A M 2009 *Astrophys. J.* **703** 1044
[6] Arnaud K A 1996 *Astronomical Data Analysis Software and Systems V* (*ASP Conf. Ser.* vol 101) ed Jacoby G H and Barnes J (San Francisco: Astron. Soc. Pac.) p. 17
[7] Verner D A, Ferland G J, Korista K T and Yakovlev D G 1996 *Astrophys. J.* **465** 487
[8] Wilms J, Allen A and McCray R 2000 *Astrophys. J.* **542** 914
[9] Nobili L, Turolla R and Zane S 2008 *Mon. Not. R. Astron. Soc.* **386** 1527
[10] Nobili L, Turolla R and Zane S 2008 *Mon. Not. R. Astron. Soc.* **389** 989
[11] Kuiper L, Hermsen W, den Hartog P R and Urama J O 2012 *Astrophys. J.* **748** 133
[12] Viganò D, Rea N, Pons J A, Perna R, Aguilera D N and Miralles J A 2013 *Mon. Not. R. Astron. Soc.* **434** 123
[13] Camilo F, Kaspi V M, Lyne A G, Manchester R N, Bell J F, D'Amico N, McKay N P F and Crawford F 2000 *Astrophys. J.* **541** 367
[14] Camilo F, Ransom S M, Halpern J P and Reynolds J 2007 *Astrophys. J.* **666** 93
[15] Rea N *et al* 2013 *Astrophys. J.* **775** L34
[16] Pons J A and Rea N 2012 *Astrophys. J.* **750** L6
[17] Li X, Levin Y and Beloborodov A M 2016 *Astrophys. J.* **833** 189
[18] Pons J A and Geppert U 2007 *Astron. Astrophys.* **470** 303
[19] Geppert U, Page D and Zannias T 1999 *Astron. Astrophys.* **345** 847
[20] Viganò D and Pons J A 2012 *Mon. Not. R. Astron. Soc.* **425** 2487
[21] Shabaltas N and Lai D 2012 *Astrophys. J.* **748** 148
[22] Torres-Forné A, Cerdá-Durán P, Pons J A and Font J A *Mon. Not. R. Astron. Soc.* **456** 3813
[23] Pons J A, Link B, Miralles J A and Geppert U 2007 *Phys. Rev. Letters* **98** id. 071101
[24] Perna R and Pons J A 2011 *Astrophys. J.* **727** L51